

Published in final edited form as:

J Dermatol Sci. 2013 December ; 72(3): . doi:10.1016/j.jdermsci.2013.08.003.

Altered sphingoid base profiles predict compromised membrane structure and permeability in atopic dermatitis

Nicolas Loiseau^{1,2}, Yasuko Obata³, Sam Moradian¹, Hiromu Sano³, Saeko Yoshino⁴, Kenichi Aburai⁴, Koza Takayama³, Kazutami Sakamoto^{4,5}, Walter M. Holleran¹, Peter M. Elias¹, and Yoshikazu Uchida^{1,*}

¹Department of Dermatology, School of Medicine, University of California, San Francisco, Veteran Affairs Medical Center, and Northern California Institute for Research and Education, San Francisco, CA USA

²Integrative Toxicology and Metabolism, Pôle de Toxicologie Alimentaire Laboratoire de Pharmacologie et Toxicologie Institut National de la Recherche Agronomique INRA UR66, Toulouse France

³Department of Pharmaceutics, Hoshi University, Tokyo Japan

⁴Department of Pure and Applied Chemistry, Tokyo University of Science, Noda, Chiba Japan

⁵Faculty of Pharmacy Chiba Institute of Science, Choshi, Chiba, Japan

Abstract

Background—Ceramide hydrolysis by ceramidase in the stratum corneum (SC) yields both sphingoid bases and free fatty acids (FFA). While FFA are key constituents of the lamellar bilayers that mediate the epidermal permeability barrier, whether sphingoid bases influence permeability barrier homeostasis remains unknown. Pertinently, alterations of lipid profile, including ceramide and ceramidase activities occur in atopic dermatitis (AD).

Object—We investigated alterations in sphingoid base levels and/or profiles (sphingosine to sphinganine ratio) in the SC of normal vs. AD mice, a model that faithfully replicates human AD, and then whether altered sphingoid base levels and/or profiles influence(s) membrane stability and/or structures.

Methods—Unilamellar vesicles (LV), incorporating the three major SC lipids (ceramides/FFA/cholesterol) and different ratios of sphingosine/sphinganine, encapsulating carboxyfluorescein, were used as the model of SC lipids. Membrane stability was measured as release of carboxyfluorescein. Thermal analysis of LV was conducted by Differential scanning calorimetry (DSC).

Results—LV containing AD levels of sphingosine/sphinganine (AD-LV) displayed altered membrane permeability vs. normal-LV. DSC analyses revealed decreases in orthorhombic structures that form tightly-packed lamellar structures in AD-LV.

© 2013 Japanese Society for Investigative Dermatology. Published by Elsevier Ireland Ltd. All rights reserved.

*Corresponding Author: Yoshikazu Uchida, Ph.D., Dermatology Service (190), Veterans Affairs Medical Center, 1700 Owen Street, Room 326, San Francisco, CA 94158 U.S.A., 4150 Clement Street, San Francisco, CA 94121 U.S.A., Tel: (415) 575-0524, Fax: (415) 750-2106, uchiday@derm.ucsf.edu.

The authors have no conflict of interest to declare

Publisher's Disclaimer: This is a PDF file of an unedited manuscript that has been accepted for publication. As a service to our customers we are providing this early version of the manuscript. The manuscript will undergo copyediting, typesetting, and review of the resulting proof before it is published in its final citable form. Please note that during the production process errors may be discovered which could affect the content, and all legal disclaimers that apply to the journal pertain.

Conclusion—Sphingoid base composition influences lamellar membrane architecture in SC, suggesting that altered sphingoid base profiles could contribute to the barrier abnormality in AD.

Keywords

atopic dermatitis; barrier; ceramide; sphingosine

INTRODUCTION

The outermost layer of the epidermis, the stratum corneum (SC), serves as the principal barrier against excessive transcutaneous water loss, while simultaneously blocking ingress of microbial pathogens, allergens and other xenotoxic agents [1, 2]. The epidermal permeability barrier localizes to the extracellular domains of the SC, where stacks of broad lamellar bilayers, enriched in free fatty acids (FFA), cholesterol and ceramides (Cer), account for barrier competence [3–5]. Most abundant among these lipids are Cer, which account for about 50% of total SC lipid mass, and comprise at least ten different species, including epidermal-unique omega(ω)-O-acylated forms, which are critical contributors to the organization of these lamellar bilayers [6, 7]. Much of this Cer heterogeneity is determined by differences in sphingoid base and amide-linked fatty acid structures [7]. Yet, it remains unknown how each lipid type influences barrier function.

Sphingoid bases are long-chain amino alcohols that are both immediate precursors, as well as catabolites of Cer, generated within the SC by one or more ceramidases [8–10]. While these molecules show amphiphilic, detergent-like properties that account for their potent *in vitro* antimicrobial activity [11, 12], they also inhibit both protein kinase C [13, 14] and phosphatidate phosphohydrolase [15] activities. Although the free sphingoid base content of nucleated mammalian cells, including keratinocytes, is relatively low [16], levels rise to 5–6 mol % of total lipids in SC, amounts still lower than the three major SC lipids (Cer, FFA, and cholesterol in Table 1). Prior studies demonstrated that supraphysiological levels of sphingosine (So) (>10 mol %), when added to phospholipid-cholesterol model membranes, increase phase transition temperatures and enthalpy [17], leading to our current hypothesis that sphingoid base content could also influence membrane stability in the SC. Yet, nothing is known about how sphingoid base profiles dictate function in normal SC; nor whether abnormalities in sphingoid base content and composition (distribution) contribute to the abnormal permeability barrier in atopic dermatitis (AD).

AD is a chronic, inflammatory skin disease that until recently was attributed to abnormalities in adaptive and innate immunity [18]. Recent evidence suggests that AD instead is often initiated by inherited abnormalities that compromise either SC structural or enzymatic proteins [19, 20]. The diminished content of specific species of EOS (Cer 1) and NP (Cer 3) are characteristic downstream features that contribute to the abnormal permeability barriers not only in human [21–23], but also in canine [24] AD. Conversely, Cer replenishment appears to improve barrier function and clinical status in AD [25, 26]. In addition, sphingosine content and acidic (but not alkaline) ceramidase activity decreased in a part of the SC fraction in human [27]. This prior study assessed neither whole SC nor another sphingoid base species, *i.e.*, sphinganine (Sa) content. We previously reported that epidermal specific alkaline ceramidase is highly expressed in the late stages of differentiation, and its activity persist in the SC [28]. Moreover, ceramidase activities are elevated in AD patient skin [29], while pertinently glycerophospholipids derived from *Staphylococcus aureus* activate ceramidase generated from colonized *Pseudomonas* in AD patients. Both of these microbial pathogens often colonize in AD patients [30]. Hence, it is unclear whether decreased acidic ceramidase activities significantly influence ceramide hydrolysis in the SC of AD.

Given that prominent alterations in sphingoid base content occur in AD [27], we hypothesized that modulations in sphingoid base levels and/or ratios could influence lamellar membrane structure, thereby contributing to altered permeability barrier function in AD. However, reported lipid biochemical data for humans with AD have relied upon topical solvent extracts or tape/cyanoacrylate strippings, which may incompletely sample the SC. Prior studies demonstrated that alterations of lipid lamellar structures become evident in the lower stratum corneum [31], suggesting that abnormal barrier structures in the lower part of the stratum corneum affect barrier function. Therefore, it is important to use whole SC rather than a part of the SC for obtaining basal sphingoid base profile to assess the influences of sphingoid base composition on membrane structures. We analyzed whole SC instead of a part of the stratum corneum to obtain basis of sphingoid profile in order to study the roles of sphingoid bases in lamellar membrane structures in the SC. We first investigated whether the alterations in epidermal lipid content and composition that have been reported for human AD occur in lipid extracts of whole SC from our AD mouse model [32–34]. After showing that the mouse model replicates reported lipid biochemical abnormalities in human AD, we analyzed and quantitated sphingoid base levels in these whole SC extracts, and then investigated the role of sphingoid base variability in membrane permeability and organization, in unilamellar vesicles (LV) reconstituted with lipids that reflect normal or AD SC. Our studies show that *i*) sphingoid bases influence membrane permeability, and *ii*) altered ratios of So to Sa attenuate lamellar membrane stability and disturb lamellar membrane organization in AD SC.

MATERIALS AND METHODS

Materials

N-Octadecanoyl-D-*erythro*-sphingosine (N-stearoylsphingosine) was purchased from Matreya (Pleasant Gap, PA). Cholesterol, palmitic acid and sphingoid bases were purchased from Matreya or Sigma-Aldrich (St. Louis, Mo.) or generously supplied by Takasago International (Tokyo, Japan). Other chemicals used were reagent grade.

AD model mice

AD model mice are prepared as described previously [32]. All animal procedures were approved by the Animal Studies Subcommittee of the San Francisco Veterans Affairs Medical Center and performed in accordance with their guidelines.

Lipids extraction

SC was isolated from skin by the incubation with trypsin in phosphate-buffered saline as described previously [35], followed by extracting lipids by Folch's method [36]. Lipid extracts were fractionated into cholesterol, FFA and ceramide by high-performance thin layer chromatography [37]. Lipids were visualized after treatment with cupric acetate–phosphoric acid, and heating to 160 C for 15 minutes followed by quantitation by scanning densitometry as we described previously [37]. Lipid content was reported as μg of total lipids/mg dry SC weight. Molecular weights used for calculation are EOS (Cer 1), 1011.96; other ceramides, 649.64; stearic acid for FFA, 284.27; and cholesterol, 386.35 to prepare LV.

Sphingosine and sphinganine quantification

Sphingosine (So) and sphinganine (Sa) content was assessed according to Min JK *et al.* [16]. Briefly, sphingoid base such as So and Sa were converted to o-phthalaldehyde derivatives. Sphingoid base o-phthalaldehyde derivatives were separated on C18 reverse phase HPLC column (Luna C18(2), 250 \times 4.6 mm, 5 μm , Phenomenex, Torrance, CA) using

methanol:water (9:1) (v/v) with a 1 ml/min flow. Fluorescence intensity was monitored at Ex 360 nm and Em 430 nm.

Unilamellar Vesicle (LV) liposome preparation

Unilamellar Vesicle (LV) liposome preparations were prepared as previously reported [38] with modifications. Ceramide, cholesterol, palmitic acid, and sphingoid base were dissolved in chloroform/methanol (2:1, v/v), and the mixture was evaporated to dryness under a stream of nitrogen. The samples were hydrated in 20 mM PIPES, 20 mM carboxyfluorescein (CF), pH 7.4, followed by freeze-thawing five times. LV (100 nm) was prepared using Avanti® Mini-Extruder following the manufacturer's protocol (Avanti Polar Lipids, Inc., Alabaster, AL). Briefly, hydrated samples were extruded between two syringes through a 100 nm polycarbonate filter 20 times and then fractionated on a 5 cm Sephadex G50 column.

Microscopy

The size and homogeneity of LV were examined by electron microscopy (Zeiss 10A, Carl Zeiss, Thornwood, NY). Anisotropy is studied using a Polarizing microscopy.

Measurement of LV permeability

LV (50 mM of total lipids) in PBS were incubated with or without sodium dodecyl sulfate (SDS), sphingoid base (1 nM-100 mM) at room temperature. In some experiments, LV were incubated at 50 and 70°C. The fluorescence intensity of aliquots of diluted liposomal suspension was measured at Ex 497 nm and Em 518 nm (Shimadzu spectrofluorimeter, RF-5301, Kyoto, Japan). The results were identified as CF release (%CFR) over time (t) in minutes, *i.e.*, $\%CFR = CFR_{min} + CFR_{max} / (1 + 10^{\exp((\log(CFR_{50}) - \log[SDS]) \times HillSlope)})$. CFR_{min} and CFR_{max} are initial fluorescence intensity and total CF release. The relative permeability of different LV compositions was compared based upon the point at which 50% of the dye had been released (CF50). A higher CF50 value corresponds with a lower relative membrane permeability. Mean \pm SD (n=3).

Thermal Analysis

Thermal analysis was conducted by Differential scanning calorimetry (DSC 8230, Rigaku Co., Tokyo, Japan) at a scan rate of 1.0°C/min over the temperature range from 15°C to 60°C, as previously reported [39].

Statistical Analyses

Statistical comparisons were performed using an unpaired Student *t* Test.

RESULTS

Altered Cer and sphingoid base profiles in normal vs. AD murine SC

Since prior studies on human AD relied upon either solvent swabbing or tape/cyanoacrylate stripping that incompletely sample all levels of the SC, we first assessed lipid profiles in whole SC from mice with an established AD-like dermatosis model that replicates many features of human AD [32]. We then compared the content and composition of ceramides (Cer), free fatty acids, cholesterol, and sphingoid bases in the SC of these mice to the reported lipid abnormalities in human AD. While total Cer content did not change, acylceramide (EOS [Cer1]) and NP (Cer 3) levels declined significantly in the SC of murine AD (Table 1), mirroring changes that occur in humans with AD [22, 40]. Moreover, similar to human AD, FFA content also declined modestly in AD mouse SC, while cholesterol levels increased (Table 1), alterations that again reflect similar changes in human AD. Thus,

AD mice display abnormalities in Cer and FFA profiles that closely resemble known lipid biochemical abnormalities in the SC of humans with AD.

We next assessed sphingoid base levels in the SC of normal and AD mice. Two major sphingoid base species, C18-sphingosine (C18-So) and C18-sphinganine (C18-Sa), were detected in both normal and AD murine SC (Table 1). While C18-So levels increased significantly (1.6-fold vs. normal; $p < 0.01$), C18-Sa content instead decreased significantly (by 57% of normal mouse SC [$p < 0.01$]) in the SC of AD mice. These changes significantly alter the molecular ratio of C18-So to C18-Sa in AD mouse SC; *i.e.*, from 5.4 in normal-SC to 14.3 in AD-SC ($p < 0.01$, Table 1) (alterations in the ratios of individual sphingoid bases also occur in the SC of human AD [private communications with Cho Y, Kyung Hee University, South Korea]). Together, these studies demonstrate that not only Cer, but also sphingoid base levels, as well as their molecular ratios, change in the SC of AD mice. Because of similarities in lipid profiles of mouse model and human AD, we utilized these SC lipid profiles, which were based upon extracts of whole SC, as the basis for the model lipid studies described below.

Sphingoid base content/composition predict membrane permeability of normal SC

To investigate whether sphingoid base content and composition influence membrane permeability in normal SC, we prepared unilamellar vesicles (LV), composed of cholesterol; FFA (palmitic acid); and ceramide (N-stearoylsphingosine), with or without added So and/or Sa, at concentrations and distributions comparable to normal mouse SC (Table 1). Ultrastructural analysis demonstrated that all LVs, with or without added sphingoid base(s), were homogeneous in size (Fig. 1, insert). Moreover, all LVs, whether prepared with or without sphingoid base(s), were stable, based upon the kinetics of 2,5-carboxyfluorescein (CFC) release over 3 days at 15–22°C (not shown). However, when LV were stressed by exposure to low concentrations of the anionic surfactant, sodium dodecyl sulfate (SDS), CFC release increased progressively both over time and as SDS concentrations increased (Fig. 1A). Likewise, another external stressor; *i.e.*, heat stress, also attenuated membrane stability, releasing CFC from LV in a time and dose-dependent manner (Fig. 1B).

Membrane stability declined further in LV that contained either sphingosine (C-18 So) or sphinganine (C-18 Sa) alone at concentrations found in normal SC (Fig. 1A and Table 2). Yet, not one, but rather two sphingoid bases (C18-So and C18-Sa) are present in normal SC (Table 1). Hence, we next assessed alterations in membrane permeability in LV reconstituted with relevant concentrations of both So and Sa. In contrast to LV that contained a single sphingoid base, LV stabilized when the two sphingoid base species were incorporated into LV membranes at the amounts found in normal SC (Table 2). Together, these results show that membrane stability declines in LV reconstituted with either So or Sa alone, while inclusion of both So and Sa at a ratio found in normal SC stabilizes these membranes.

Alterations in sphingoid base content/distribution predict abnormal membrane permeability in AD

Although sphingosine (So) levels are known to decline in a part of the SC of human AD [27], other sphingoid base, *i.e.*, sphinganine (Sa), content of the whole SC has not yet been characterized in AD. While So content increases (1.6-fold higher), we found here that Sa content decreases (1.8-fold lower) in the whole SC of murine AD than in normal SC (Table 1). Therefore, we next assessed whether such AD-type alterations in sphingoid base composition destabilize LV membranes. For the initial group of studies, we employed LV reconstituted with a normal ratio of cholesterol, FFA, and Cer (+/- added sphingoid bases) in order to exclude a separate influence of changes in the content of these lipids on

membrane stability (see below for further studies on the separate effects of altered cholesterol/FFA on membrane stability). In these studies, we compared CFC release rates from LV that incorporated So and Sa at concentrations/ratios found in AD SC, to LV containing a normal sphingoid base profile. Although LV prepared with AD sphingoid bases remained stable over 3 days at 15–22°C, membrane stability declined in these LV, following exposure to SDS (Table 2). Moreover, AD levels of sphingoid bases compromised membrane permeability in LV not only following exposure of LV to SDS, but also following application to a second, unrelated stressor; *i.e.*, elevated temperatures. Before raising the temperature, CFC release increased slowly in LV containing normal sphingoid base profiles (Fig. 1B, closed triangles), but CFC release increased much more rapidly in LV containing AD levels of So and Sa as temperature increased (Fig. 1B, open circles). Together, these results demonstrate that AD-type sphingoid base profiles destabilize otherwise normal LV membranes.

AD profiles of cholesterol and FFA diminish membrane stability separately, as well as additively with sphingolipid bases

Cholesterol and FFA levels are altered in the SC of both human AD [22, 40] and AD mice (Table 1). Hence, we next assessed whether an increase in cholesterol and a decrease in FFA that mimics human and murine AD alter(s) the permeability of LV. Then, we assessed whether these alterations are additive to the defective permeability produced by AD profiles of the sphingoid bases alone. AD levels of cholesterol and FFA content further (additively) compromised membrane stability in these LV (Table 3). These results show that addition of AD levels of sphingoid bases additively diminishes membrane stability.

Sphingoid bases regulate membrane permeability by structural, rather than by detergent-like mechanisms

Because sphingoid bases are amphiphilic lipids, the sphingoid base-induced changes in membrane permeability described above could, in theory, reflect detergent activity, rather than an impact of these lipids on membrane structure. To determine whether altered membrane stability reflects detergent activity, we next assessed whether addition of exogenous So/Sa to LV alters membrane stability. We applied exogenous So and/or Sa to suspensions of pre-prepared LV prepared without So and/or Sa. The CF50 (mM) of both exogenous So and Sa was 1–1.2 mM (Fig. 2). Since the So or Sa content in the LV is <10 μM, the observed alterations in membrane permeability, induced by altered sphingoid base profiles in AD, likely do not reflect detergent effects of the released sphingoid bases from LV.

We next assessed the alternate possibility; *i.e.*, whether the sphingoid bases influence membrane structure. Differential scanning calorimetry (DSC) analysis revealed a comparable phase transition in LV, containing So and/or Sa at either normal or AD levels (49.8 ± 0.96 °C or 49.5 ± 4.29 °C; not statistically different), respectively (Fig. 3A). Moreover, polarizing microscope showed maltese cross structures that represent the formation of lamellar membranes appearing membrane structure between temperatures of 45° to 60°C in both normal and AD-LV (Fig. 3C). But DSC thermograms of LV with So and Sa at normal levels showed an additional shoulder at around 40 °C that disappeared in LV that contained So/Sa at AD levels (Fig. 3A). This peak corresponds to a phase transition that reflects orthorhombic packing of tightly-packed lamellar structures [41]. In addition, the enthalpy of these membranes, which representing their internal energy, was significantly greater in LV with a normal base profiles than the enthalpy of LV prepared with AD levels of So/Sa (Fig. 3B), indicating higher membrane stability. Together, these results show that the sphingoid bases influence membrane permeability through their impact on membrane structural organization.

DISCUSSION

Human AD shows both chronic inflammation and an abnormal permeability barrier, with the latter now assumed to be the primarily 'driver' of disease pathogenesis [42]. Though mutations in structural proteins of the corneocyte underlie many cases of human AD, the permeability barrier abnormality in filaggrin-deficient epidermis localizes to the extracellular matrix, where lamellar bilayer structure is abnormal [43]. While the reduced EOS (Cer 1) and NP (Cer 3) levels in AD have been proposed to be an important contribution to the barrier abnormality [21, 22, 40], sphingoid base production is altered in AD [27, 29]. Sphingoid bases are generated by the hydrolysis of Cer by one or more isoforms of ceramidase. Our prior studies demonstrated that ceramidases are enriched in SC [28]. Furthermore, we recently showed by *in situ* zymography that these ceramidases are functionally active in normal human SC [10]. It was noted in a prior study that a virulent microbial pathogen, *Staphylococcus aureus* that often colonizes in AD skin, as well as *Pseudomonas*, produce ceramidase activators (*i.e.*, glycerophospholipids) and/or ceramidases that could alter sphingoid base levels and ratios in AD epidermis [30]. In addition, the hyperplasia and inflammation in AD could modify sphingolipid metabolism in AD. Hence, not only base metabolism, but also pathogen-induced abnormalities likely occur in AD epidermis.

Yet, while the enzymatic capacity to generate these bases is present in both normal and AD SC, the consequences of the altered sphingoid base profile for membrane structure and function in AD remains unknown. Moreover, whether the altered sphingoid base content of AD could contribute to the barrier abnormality in human AD is not yet known. To address these issues, we demonstrated here first, that sphingoid bases play an important structural role in stabilizing model membranes that mimic normal SC. Specifically, the two major sphingoid bases (So and Sa) must be present at a ratio that reflects normal SC to stabilize membrane bilayer structure in this *in vitro* model. Conversely, we demonstrated that the abnormal profiles/ratios of sphingoid bases that occur in AD instead destabilize (permeabilize) the same model lipid membranes. These abnormalities appeared as sphingosine (So) to sphinganine (Sa) ratios began to approach those found in the SC of AD model mice, and were accelerated by exposure to either chemical (detergent) or heat stress. We chose SDS as one stressor to bring out functional abnormalities, because it is widely used as a detergent in topical formulations which both normal and AD human subjects frequently are exposed to. Our results suggest that SDS exposure from soaps or skin care formulation could further modify membrane permeability in AD patients by attenuating barrier function. Moreover, heat stress, which simulates skin exposure during bathing in hot water, brought out the same functional abnormality.

The altered sphingoid base ratios employed here were based upon lipid extracts from the SC of our recently established AD-like mouse model, which mimics human AD functionally, structurally, and immunologically [32, 33, 44]. Importantly, lipid extracts from the SC of AD mice showed not only reduced levels of specific Cer species, EOS (Cer1) and NP (Cer 3), but also alterations in the ratio of sphingosine to sphinganine that again resemble known alterations in human AD (private communications with Cho Y, Kyung Hee University, South Korea). In these studies, we utilized sphingoid base profiles based upon the mouse rather than human data, because these levels represent base levels in whole SC, while published human data on sphingoid base levels inevitably derive from either solvent extracts or pooled tape or cyanoacrylate strippings that do not sample whole SC [27]. Moreover, lipid extracts from whole SC of AD mice displayed similar alterations of Cer, FFA and cholesterol profiles as occur in human AD [40]. Thus, an altered sphingoid base molecular ratio, coupled with altered Cer:cholesterol:FFA ratios, likely contributes to the known attenuation of epidermal permeability barrier function that occurs in AD. Yet, it must be

noted that our model LV system did not fully replicate *in vivo* conditions, because it did not include the full range of Cer in SC, which includes a family of at least ten species [45–47]. Nevertheless, our study strongly suggests that not only reduced specific species of Cer (EOS and NP), but also alterations in the profile of Cer downstream metabolites; *i.e.*, sphingoid bases, regulate the integrity of lamellar membranes in AD. Moreover, changes in cholesterol and FFA content that occur in AD separately and additively perturbed membrane permeability in our membrane system. In summary, although the cholesterol and FFA content of SC are substantially greater (cholesterol >5~7-fold and FFA >8~11-fold) than the sphingoid base content of SC (Table 1), our results show that *the sphingoid bases, though only a minor bulk lipid species, contribute to the structural organization and permeability of model membranes.*

Finally, our studies provide mechanistic insights about how sphingoid bases influence membrane structure and permeability. DSC analysis demonstrated that a structural abnormality, rather than the potential detergent activity of these bases accounts for altered permeability in AD model membrane. Physico-chemical assessments using differential scanning calorimeter and polarized microscopy revealed that LV with not only normal, but also AD sphingoid base profiles displayed a normal profile of phase transition temperatures. Yet, pertinently, only LV with normal sphingoid bases showed evidence of orthorhombic packing structures. Our recent studies confirmed these structural changes, including the presence/absence of orthorhombic structures, by X-ray diffraction analysis (not shown). Prior studies demonstrated the coexistence of hexagonal and tightly packed orthorhombic structures in the SC [41, 48, 49]. The latter orthorhombic structures are thought to contribute to the reduced permeability and barrier competence of normal SC [41, 48, 49]. Recent report suggests that addition of a monounsaturated fatty acid increases hexagonal structures in model membranes [50], supporting these DSC studies, *i.e.*, an increase in the ratio of sphingosine (monosaturated) levels to sphinganine (saturated) decreases in orthorhombic structures. However, it remains to be determined how an increase in desaturated species of sphingoid bases alter membrane structure and permeability in AD, while conversely how different ratios of So to Sa improve membrane stability. Changes not only in sphingoid base profile, but also Cer species, as well as altered ratios of cholesterol and FFA could (additively) alter lamellar membrane structures. Pertinently, recent studies suggest that the shorter carbon chain lengths of Cer in AD could contribute to attenuations of permeability barrier function [51]. Nevertheless, together with our functional assessments using the carboxyfluorescein release assay, our results show that LV with normal sphingoid base profiles form more tightly packed lamellar structures that lead to less permeable membrane than membranes reconstituted with AD levels of the bases. Hence, abnormal sphingoid base species likely contribute to the barrier abnormality in AD.

Acknowledgments

Funding: Department of Veterans Affairs (USA) and National Institute of Health

The authors thank Ms. Debra Crumrine for ultrastructural analysis (University of California San Francisco) and Dr. Masahiko Abe for technical advice (Tokyo University of Science, Noda, JAPAN). The author acknowledges the superb editorial assistance of Ms. Joan Wakefield. The authors gratefully acknowledge the support of the Medical Research Services of the Veterans Affairs Medical Center, San Francisco (Merit Review Grant to PME) and National Institutes of Health (Grant AR051077 and AR062025 to YU).

Abbreviations

AD	atopic dermatitis
CFC	2,5-carboxyfluorescein

Cer	ceramide
DSC	Differential scanning calorimetry
FFA	free fatty acids
Sa	sphinganine
So	sphingosine
LV	unilamellar vesicles
SDS	sodium dodecyl sulfate
SC	stratum corneum

References

1. Elias PM, Menon GK. Structural and lipid biochemical correlates of the epidermal permeability barrier. *Advances in Lipid Research*. 1991; 24:1–26. [PubMed: 1763710]
2. Elias PM. Stratum corneum defensive functions: an integrated view. *J Invest Dermatol*. 2005; 125:183–200. [PubMed: 16098026]
3. Bouwstra J, Pilgram G, Gooris G, Koerten H, Ponec M. New aspects of the skin barrier organization. *Skin Pharmacol Appl Skin Physiol*. 2001; 14:52–62. [PubMed: 11509908]
4. Schürer NY, Plewig G, Elias PM. Stratum corneum lipid function. *Dermatologica*. 1991; 183:77–94. [PubMed: 1743378]
5. Holleran WM, Takagi Y, Uchida Y. Epidermal sphingolipids: Metabolism, function, and role(s) in skin disorders. *FEBS Letters*. 2006; 23:5456–5466. [PubMed: 16962101]
6. Bouwstra JA, Honeywell-Nguyen PL, Gooris GS, Ponec M. Structure of the skin barrier and its modulation by vesicular formulations. *Prog Lipid Res*. 2003; 42:1–36. [PubMed: 12467638]
7. Uchida Y, Holleran WM. Omega-O-acylceramide, a lipid essential for mammalian survival. *J Dermatol Sci*. 2008; 51:77–87. [PubMed: 18329855]
8. Wertz PW, Downing DT. Ceramidase activity in porcine epidermis. *FEBS Lett*. 1990; 268:110–112. [PubMed: 2384145]
9. Houben E, Uchida Y, Nieuwenhuizen WF, De Paepe K, Vanhaecke T, Holleran WM, et al. Kinetic characteristics of acidic and alkaline ceramidase in human epidermis. *Skin Pharmacol Physiol*. 2007; 20:187–194. [PubMed: 17396053]
10. Lin TK, Crumrine D, Ackerman LD, Santiago JL, Roelandt T, Uchida Y, et al. Cellular Changes that Accompany Shedding of Human Corneocytes. *J Invest Dermatol*. 2012; 132:2430–2439. [PubMed: 22739796]
11. Bibel DJ, Aly R, Shinefield HR. Antimicrobial activity of sphingosines. *J Invest Dermatol*. 1992; 98:269–273. [PubMed: 1545135]
12. Drake DR, Brogden KA, Dawson DV, Wertz PW. Thematic review series: skin lipids. Antimicrobial lipids at the skin surface. *J Lipid Res*. 2008; 49:4–11. [PubMed: 17906220]
13. Hannun YA, Loomis CR, Bell RM. Protein kinase C activation in mixed micelles. Mechanistic implications of phospholipid, diacylglycerol, and calcium interdependencies. *J Biol Chem*. 1986; 261:7184–7190. [PubMed: 3711083]
14. Arnold RS, Newton AC. Inhibition of the insulin receptor tyrosine kinase by sphingosine. *Biochem*. 1991; 30:7747–7754. [PubMed: 1651108]
15. Mullmann TJ, Siegel MI, Egan RW, Billah MM. Sphingosine inhibits phosphatidate phosphohydrolase in human neutrophils by a protein kinase C-dependent mechanism. *J Biol Chem*. 1991; 266:2013–2016. [PubMed: 1989967]
16. Min JK, Yoo HS, Lee EY, Lee WJ, Lee YM. Simultaneous quantitative analysis of sphingoid base 1-phosphates in biological samples by o-phthalaldehyde precolumn derivatization after dephosphorylation with alkaline phosphatase. *Anal Biochem*. 2002; 303:167–175. [PubMed: 11950216]

17. Contreras FX, Sot J, Alonso A, Goni FM. Sphingosine increases the permeability of model and cell membranes. *Biophys J*. 2006; 90:4085–4092. [PubMed: 16533839]
18. Boguniewicz M, Leung DY. Atopic dermatitis: a disease of altered skin barrier and immune dysregulation. *Immunol Rev*. 2011; 242:233–246. [PubMed: 21682749]
19. Hou M, Man M, Man W, Zhu W, Hupe M, Park K, et al. Topical hesperidin improves epidermal permeability barrier function and epidermal differentiation in normal murine skin. *Exp Dermatol*. 2012; 21:337–340. [PubMed: 22509829]
20. Elias PM, Steinhoff M. “Outside-to-inside” (and now back to “outside”) pathogenic mechanisms in atopic dermatitis. *J Invest Dermatol*. 2008; 128:1067–1070. [PubMed: 18408746]
21. Imokawa G, Abe A, Jin K, Higaki Y, Kawashima M, Hidano A. Decreased level of ceramides in stratum corneum of atopic dermatitis: an etiologic factor in atopic dry skin? *J Invest Dermatol*. 1991; 96:523–526. [PubMed: 2007790]
22. Bleck O, Abeck D, Ring J, Hoppe U, Vietzke JP, Wolber R, et al. Two ceramide subfractions detectable in Cer(AS) position by HPTLC in skin surface lipids of non-lesional skin of atopic eczema. *J Invest Dermatol*. 1999; 113:894–900. [PubMed: 10594727]
23. Macheleidt O, Kaiser HW, Sandhoff K. Deficiency of epidermal protein-bound omega-hydroxyceramides in atopic dermatitis. *J Invest Dermatol*. 2002; 119:166–173. [PubMed: 12164940]
24. Yoon JS, Nishifuji K, Sasaki A, Ide K, Ishikawa J, Yoshihara T, et al. Alteration of stratum corneum ceramide profiles in spontaneous canine model of atopic dermatitis. *Exp Dermatol*. 2011; 20:732–736. [PubMed: 21649737]
25. Chamlin SL, Frieden IJ, Fowler A, Williams M, Kao J, Sheu M, et al. Ceramide-dominant, barrier-repair lipids improve childhood atopic dermatitis. *Arch Dermatol*. 2001; 137:1110–1112. [PubMed: 11493117]
26. Sugarman JL, Parish LC. Efficacy of a lipid-based barrier repair formulation in moderate-to-severe pediatric atopic dermatitis. *J Drugs Dermatol*. 2009; 8:1106–1111. [PubMed: 20027938]
27. Arikawa J, Ishibashi M, Kawashima M, Takagi Y, Ichikawa Y, Imokawa G. Decreased levels of sphingosine, a natural antimicrobial agent, may be associated with vulnerability of the stratum corneum from patients with atopic dermatitis to colonization by *Staphylococcus aureus*. *J Invest Dermatol*. 2002; 119:433–439. [PubMed: 12190867]
28. Houben E, Holleran WM, Yaginuma T, Mao C, Obeid LM, Rogiers V, et al. Differentiation-associated expression of ceramidase isoforms in cultured keratinocytes and epidermis. *J Lipid Res*. 2006; 47:1063–1070. [PubMed: 16477081]
29. Ohnishi Y, Okino N, Ito M, Imayama S. Ceramidase activity in bacterial skin flora as a possible cause of ceramide deficiency in atopic dermatitis. *Clin Diagn Lab Immunol*. 1999; 6:101–104. [PubMed: 9874672]
30. Kita K, Sueyoshi N, Okino N, Inagaki M, Ishida H, Kiso M, et al. Activation of bacterial ceramidase by anionic glycerophospholipids: possible involvement in ceramide hydrolysis on atopic skin by *Pseudomonas* ceramidase. *Biochem J*. 2002; 362:619–626. [PubMed: 11879188]
31. Fartasch M, Bassukas ID, Diepgen TL. Disturbed extruding mechanism of lamellar bodies in dry non-eczematous skin of atopics. *Br J Dermatol*. 1992; 127:221–227. [PubMed: 1390165]
32. Man MQ, Hatano Y, Lee SH, Man M, Chang S, Feingold KR, et al. Characterization of a hapten-induced, murine model with multiple features of atopic dermatitis: structural, immunologic, and biochemical changes following single versus multiple oxazolone challenges. *J Invest Dermatol*. 2008; 128:79–86. [PubMed: 17671515]
33. Hatano Y, Man M-Q, Uchida Y, Crumrine D, Scharschmidt TC, Kim EG, et al. Maintenance of an Acidic Stratum Corneum Prevents Emergence of Murine Atopic Dermatitis. *J Invest Dermatol*. 2009; 129:1824–1835. [PubMed: 19177139]
34. Hatano Y, Man MQ, Uchida Y, Crumrine D, Mauro TM, Feingold KR, et al. Murine atopic dermatitis responds to peroxisome proliferator-activated receptors alpha and beta/delta (but not gamma) and liver X receptor activators. *J Allergy Clin Immunol*. 2010; 125:160–169. [PubMed: 19818482]

35. Hara M, Uchida Y, Haratake A, Mimura K, Hamanaka S. Galactocerebroside and not glucocerebroside or ceramide stimulate epidermal beta-glucocerebrosidase activity. *J Dermatol Sci.* 1998; 16:111–119. [PubMed: 9459123]
36. Folch J, Lees M, Sloane Stanley GH. A simple method for the isolation and purification of total lipides from animal tissues. *J Biol Chem.* 1957; 226:497–509. [PubMed: 13428781]
37. Uchida Y, Hama H, Alderson NL, Douangpanya S, Wang Y, Crumrine DA, et al. Fatty acid 2-hydroxylase, encoded by FA2H, accounts for differentiation-associated increase in 2-OH ceramides during keratinocyte differentiation. *J Biol Chem.* 2007; 282:13211–13219. [PubMed: 17355976]
38. de la Maza A, Parra JL. Solubilizing effects caused by the nonionic surfactant dodecylmaltoside in phosphatidylcholine liposomes. *Biophys J.* 1997; 72:1668–1675. [PubMed: 9083670]
39. Otake K, Shimomura T, Goto T, Imura T, Furuya T, Yoda S, et al. Preparation of liposomes using an improved supercritical reverse phase evaporation method. *Langmuir.* 2006; 22:2543–2550. [PubMed: 16519453]
40. Di Nardo A, Wertz P, Giannetti A, Seidenari S. Ceramide and cholesterol composition of the skin of patients with atopic dermatitis. *Acta Dermato-Venereologica.* 1998; 78:27–30. [PubMed: 9498022]
41. Hatta I, Ohta N, Inoue K, Yagi N. Coexistence of two domains in intercellular lipid matrix of stratum corneum. *Biochim Biophys Acta.* 2006; 1758:1830–1836. [PubMed: 17034756]
42. Elias PM, Hatano Y, Williams ML. Basis for the barrier abnormality in atopic dermatitis: outside-inside-outside pathogenic mechanisms. *J Allergy Clin Immunol.* 2008; 121:1337–1343. [PubMed: 18329087]
43. Gruber R, Elias PM, Crumrine D, Lin TK, Brandner JM, Hachem JP, et al. Filaggrin genotype in ichthyosis vulgaris predicts abnormalities in epidermal structure and function. *Am J Pathol.* 2011; 178:2252–2263. [PubMed: 21514438]
44. Scharschmidt TC, Man MQ, Hatano Y, Crumrine D, Gunathilake R, Sundberg JP, et al. Filaggrin deficiency confers a paracellular barrier abnormality that reduces inflammatory thresholds to irritants and haptens. *J Allergy Clin Immunol.* 2009; 124:496–506. 506 e491–496. [PubMed: 19733297]
45. Wertz PW, Downing DT. Ceramides of pig epidermis: structure determination. *J Lipid Res.* 1983; 24:759–765.
46. Ponc M, Weerheim A, Lankhorst P, Wertz P. New acylceramide in native and reconstructed epidermis. *J Invest Dermatol.* 2003; 120:581–588. [PubMed: 12648220]
47. Stewart ME, Downing DT. A new 6-hydroxy-4-sphingenine-containing ceramide in human skin. *J Lipid Res.* 1999; 40:1434–1439. [PubMed: 10428979]
48. Bouwstra JA, Dubbelaar FE, Gooris GS, Ponc M. The lipid organisation in the skin barrier. *Acta Dermato-venereolog Suppl.* 2000; 208:23–30.
49. Damien F, Boncheva M. The extent of orthorhombic lipid phases in the stratum corneum determines the barrier efficiency of human skin in vivo. *J Invest Dermatol.* 2010; 130:611–614. [PubMed: 19727117]
50. Thakoersing VS, van Smeden J, Mulder AA, Vreeken RJ, El Ghalbzouri A, Bouwstra JA. Increased Presence of Monounsaturated Fatty Acids in the Stratum Corneum of Human Skin Equivalent. *J Invest Dermatol.* 2012
51. Janssens M, van Smeden J, Gooris GS, Bras W, Portale G, Caspers PJ, et al. Increase in short-chain ceramides correlates with an altered lipid organization and decreased barrier function in atopic eczema patients. *J Lipid Res.* 2012; 53:2755–2766. [PubMed: 23024286]
52. Motta S, Monti M, Sesana S, Caputo R, Carelli S, Ghidoni R. Ceramide composition of the psoriatic scale. *Biochim Biophys Acta.* 1993; 1182:147–151. [PubMed: 8357845]
53. Robson KJ, Stewart ME, Michelsen S, Lazo ND, Downing DT. 6-Hydroxy-4-sphingenine in human epidermal ceramides. *J Lipid Res.* 1994; 35:2060–2068. [PubMed: 7868984]

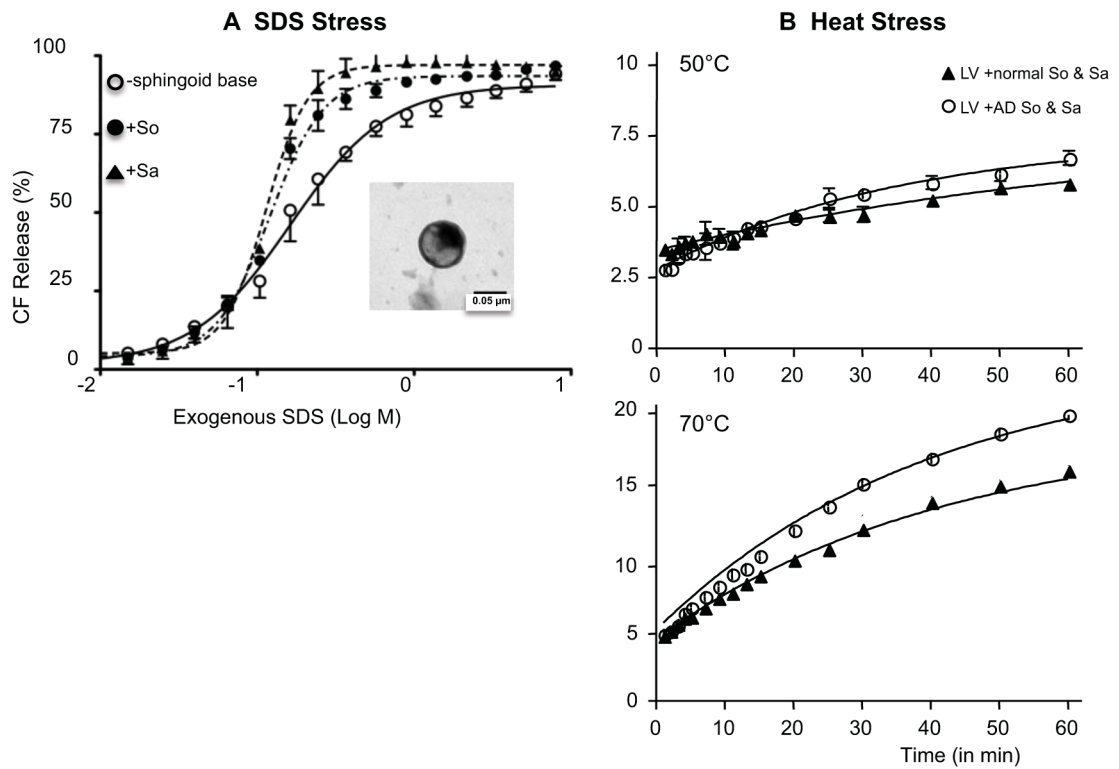


Figure 1.

Exogenous detergent (A) or heat stress (B) attenuates membrane stability of LV. Membrane stability was assessed by CF release from LV. Furthermore, LV containing either So or Sa further decreases membrane stability. Insert: Electron Microscopy (60 kV) of LV (x100K). LV solutions were stained with uranyl acetate and examined in an electron microscope (Zeiss 10A, Carl Zeiss, Thornwood, NY). Similar results were obtained when the experiment was repeated using three different liposome preparations. See details in Materials and Methods.

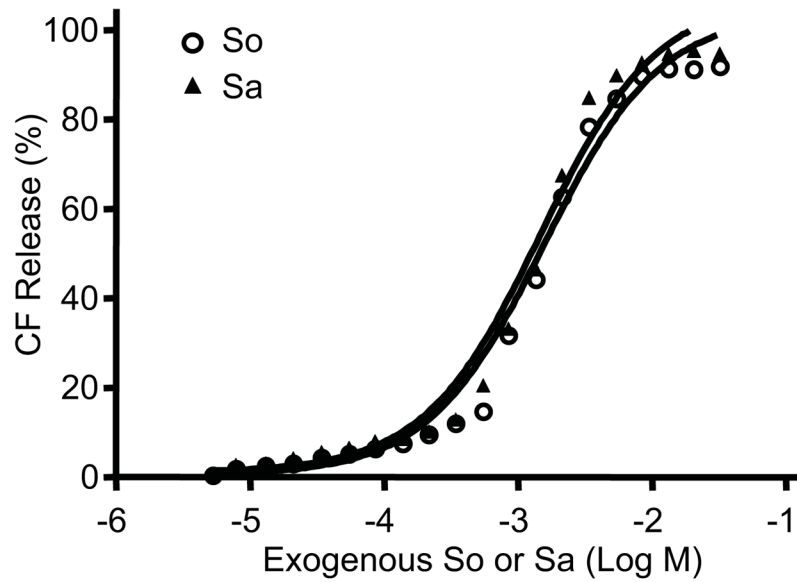


Figure 2. Neither exogenous So nor Sa, added at the highest concentrations used in the LV (Figs. 1 and 3), stimulated the release of significant amounts of CFC (as in Table 2, only = 0.2% with added So, and = 0.05% with added Sa). Similar results were obtained when the experiment was repeated using three different liposome preparations. See details in Materials and Methods.

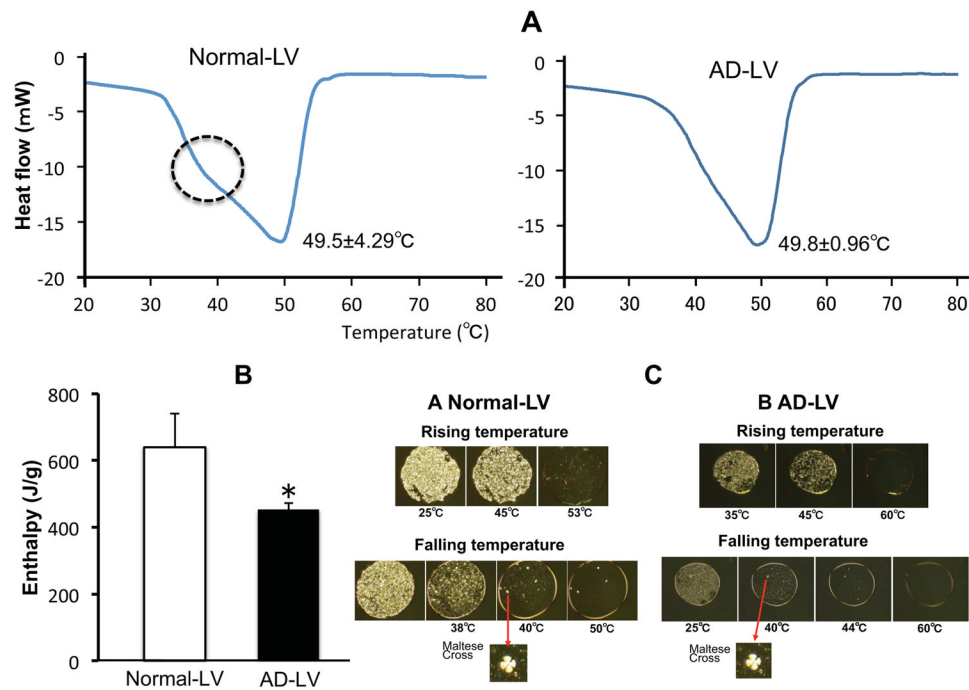


Figure 3. Thermogram of lipid model (A), enthalpy of phase transition (B), and polarized microscopy (C) of LV containing both So and Sa at normal or AD SC levels. Similar results were obtained when the experiment was repeated using five different liposome preparations. The column represents the mean \pm S.D. (n=3). NS vs. AS * $p < 0.05$. The scanning rate was $1^\circ\text{C}/\text{min}$, and PIPES buffer was used as reference. See details in Materials and Methods.

Table 1

Major lipid and sphingoid base content in the normal and atopic dermatitis (AD) model mouse stratum corneum

	Mass concentration ($\mu\text{g}/\text{mg}$ dry weight)	
	Normal	AD
Cholesterol	17.2 \pm 0.78	24.9 \pm 0.10*
Free Fatty Acids	19.3 \pm 2.92	15.1 \pm 1.38
Total Ceramides	11.0 \pm 0.80	11.5 \pm 0.30
EOS (Cer 1)	2.19 \pm 0.78	1.04 \pm 0.20*
NS (Cer 2)	3.87 \pm 0.28	3.36 \pm 0.11
NP (Cer 3)	1.59 \pm 0.15	0.74 \pm 0.12*
AS (Cer 5) [#]	3.33 \pm 0.22	2.86 \pm 0.31
AS (Cer 5) ^{##}	1.33 \pm 0.12	1.63 \pm 0.12
C18-Sphingosine	1.52 \pm 0.34	2.40 \pm 0.55
C18-Sphinganine	0.28 \pm 0.06	0.16 \pm 0.08**
Ratio C-18 So to Sa	5.43	14.3*

Cer structures are according to Motta S. *et al.* [52] and Robson KJ, *et al.* [53]: EOS (Cer 1), esterified ω -hydroxy (OH) FA with sphingosine; NS (Cer 2), non-OH FA with sphingosine; NP (Cer 3), non-OH FA with phytosphingosine; AS (Cer 5), α -OH FA with sphingosine. AS[#] are more hydrophobic species of AS, *i.e.*, containing longer amide-linked fatty acids, compared with AS^{##}. The data are indicated as the mean value \pm SD (n=4–6 mice).

* p>0.01;

** p>0.02 vs. Normal. See details in Materials and Methods.

Table 2

Alterations of membrane stability in LV containing cholesterol, palmitic acid, ceramide in normal SC and sphingoid base composition in normal and AD in response to SDS stress

	Normal		Normal		Normal		AD		AD	
	So	Sa	So and Sa	So	Sa	So and Sa	So	Sa	So and Sa	
	Mole %									
Cer (NS)	13.0	12.0	12.4	11.9	11.7	11.7	11.7	11.7	11.7	11.7
Cholesterol	34.0	33.3	34.4	33.0	32.6	32.4	32.4	32.4	32.4	32.4
Palmitic acid	53.0	50.9	52.7	50.6	50.0	49.8	49.8	49.8	49.8	49.8
C18-So	3.8			3.8	5.7	5.7	5.7	5.7	5.7	5.7
C18-Sa			0.7	0.7		0.4	0.4	0.4	0.4	0.4
Ratio So to Sa				5.43						14.3
CF50 (mM)	1.63±0.10	1.20±0.03	1.03±0.04	1.34±0.05	1.14±0.03	1.14±0.04	1.14±0.03	1.14±0.04	1.14±0.03	1.14±0.03
P value										
vs.w/o So or Sa	-	0.01	0.01	0.02	0.01	0.01	0.01	0.01	0.01	0.01
vs.normal So	0.02	-	n.s.	n.s.	n.s.	n.s.	n.s.	n.s.	n.s.	n.s.
vs.normal Sa	0.01	n.s.	n.s.	0.01	n.s.	n.s.	n.s.	n.s.	n.s.	n.s.

Hill's equation parameters were obtained fitting the data with this equation (see details in Materials and Methods). Results are indicated as the mean value ± the standard deviation from three independent analyses. CF50 indicates a concentration of SDS that releases 50% of the dye from LV. A higher CF50 value corresponds with a lower relative membrane permeability. Results are indicated as the mean value ± the standard deviation from three independent analyses. n.s., not statically significant.

Table 3

AD profiles of cholesterol and FFA diminish membrane stability additively with sphingolipid bases

	Normal		AD	
	<u>Normal SC</u>	<u>Normal SC</u>	<u>AD SC</u>	<u>AD SC</u>
	Cer, cholesterol and palmitic acid			
	Mole %			
Cer (NS)	11.9	11.7	11.5	11.5
Cholesterol	33.0	32.4	45.3	45.3
Palmitic acid	53.0	49.8	37.1	37.1
C18-So	3.8	5.7	5.7	5.7
C18-Sa	0.7	0.4	0.4	0.4
Ratio So to Sa	5.43	14.3	14.3	14.3
CF50 (mM)	1.34±0.05	1.14±0.03	0.86±0.02	0.86±0.02
vs.normal So and Sa	-	0.02	0.01	0.01
vs.AD So and Sa	0.02	-	0.02	0.02

Results are indicated as the mean value ± the standard deviation from three independent analyses.